Original scientific paper

Informacije MIDEM
Journal of Microelectronics, Electronic Components and Materials
Vol. 47, No. 1(2017), 32 – 39

2D Simulation Study of p-type TFTs with Chemically Deposited Poly-PbS Active Channel

Abimael Jiménez P.[1], Amanda Carrillo C.[1], Shehret Tilvaldyev[1], Manuel A. Quevedo L.[2], J. Antonio Muñoz G.[3]

[1]Electrical and Computer Engineering Department, Universidad Autónoma de Ciudad Juárez, Ciudad Juárez, Chihuahua, México
[2]Materials Science and Engineering Department, University of Texas at Dallas, Richardson, USA
[3]Engineering Department, Universidad de Guadalajara, Jalisco, México

Abstract: In this work, the two-dimensional (2D) numerical simulation of p-type poly-PbS TFT electrical characteristics are performed using a physically based device simulator Atlas/Silvaco. The analytical expressions of defect density models for acceptor- and donor-like traps are defined for poly-PbS thin film material deposited with chemical bath deposition technique. The parameters of defect density model are optimized based on Levenberg-Marquardt algorithm to fit simulated and experimental results of TFTs. It is shown that the spatially uniform density of defect states method used for trapped charge evaluation in Atlas gives good agreement between simulated and experimental characteristics. An important presence of deep (Gaussian) acceptor- and donor-like density of states in poly-PbS band gap is confirmed. By controlling cation (donor-like) and anion (acceptor-like) vacancies of poly-PbS films could improved the performance of p-type TFTs.

Keywords: thin film transistor, simulation, density of states, optimization, defects, chemical bath deposition

2D simulacija TFT tipa p s kemijsko nanešenim aktivnim poli-PbS kanalom

Izvleček: Dvodimenzonalne simulacije električnih karakteristik TFT tipa p s poli-PbS so opravljene s simulatorjem Atlas/Silvaco. Analitični izrazi modelov stanj defektov za akceptorje in donorje so določeni za poli-PbS material, ki je nanešen s pomočjo tehnike kemijske kopeli. Parametri modela so optimizirani s pomočjo Levenberg-Marquardt algoritma tako, da se simulacije ujemajo z eksperimentalnimi meritvami. Izkazalo se je, da se rezultati prostorsko enotne metode v Atlas-u dobro ujemajo z eksperimentalnimi rezultati. Dokazana je bila pomembnost prisotnosti globoke Gausove porazdelitve defektov. Učinkovitost TFT-ja se lahko izboljša s kontroliranim vnosom vrzeli donorskega oziroma akceptorskega tipa.

Ključne besede: tankoplastni tranzistor, simulacije, gostota stanj, optimizacija, defekti

** Corresponding Author's e-mail: abimael.jimenez@uacj.mx*

1 Introduction

Thin film transistors (TFTs) are a growing technology in the flexible and large area of electronic fields, and recently they have been investigated mainly because of their low cost of production. Also, this technology is interesting due to the recent increase in the area of displays and its use to develop high-speed devices switching pixels, electroluminescent displays, active matrix displays, image sensors, and identification systems [1, 2].

There is a variety of thin film mature technologies in the market such as hydrogenated amorphous silicon TFTs (a-Si:H TFTs), polycrystalline TFTs (particularly low temperature), and organic TFTs (OTFTs). These technologies have advantages and disadvantages. For example, although a-Si:H TFTs have good uniformity, they have the disadvantages of insuficient mobility for driving a large screen LCD at a high speed, a large threshold voltage (V_{TH}) instability due to the desorption of hydrogen, and the absence of p-type semiconductor material for

© MIDEM Society

Metal-Oxide-Semiconductor (MOS) technology. Furthermore, poly-TFTs have high mobility, but they have a drawback in that V_{TH} largely varies due to a process for crystallizing an active layer by annealing. Also, OTFTs have effcient p-type semiconductor materials, but they have the disadvantages that there is not a solution for n-type semiconductor material, they have V_{TH} in stability due to the oxidation of organic materials [3], and the organic molecules need to be aligned well at the interface or formed into large, low-defect grains, which is no trivial work.

Because some disadvantages are present in TFTs technology, researchers are looking for different options that can replace commercial materials and contribute to a better physical understanding of new materials for flexible electronics. The most important advantage of low temperature poly-TFTs technology is that it does not need expensive equipment of vacuum and high temperature processes, but printing or chemical bath deposition (CBD) techniques can still be used. In addition, CBD chalcogenide films are attractive for poly-TFTs for large area electronics given their simple fabrication, low temperature, and compatibility with most substrates. Moreover, chalcogenides materials are suitable candidates for their implementation in poly-TFTs because they have good electrical and morphological properties.

In particular, lead sulfide (PbS) chalcogenide is an important binary IV-VI semiconductor material with a direct narrow band gap [4]. It is also widely used in MOS transistors and optical devices [5], and it is one of the most widely studied semiconductos over the last decades [6, 7]. Recently, a p-type poly-TFT fabricated with PbS as semiconductor deposited by CBD technique was reported [8]. Using this technique, PbS thin films with photosensitive polycrystalline p-type conductivity can be obtained at room temperature.

Nevertheless, the CBD technique introduces structural defects (traps) during the deposition process, and numerous important electrical parameters of the TFTs are strongly affected by the density of defect states [9]. Besides, a model to predict and optimize the electrical characteristics of PbS poly-TFTs based on CBD technique is needed, so undoubtedly, device simulation tools are necessary to model and simulate a PbS poly-TFT. This work implements the 2D simulation of p-type poly-TFTs electrical characteristics using Atlas/Silvaco simulation models for Density of Defect (Trap) States (DDS).

2 Simulation of a p-type poly-PbS TFT

The simulated poly-PbS TFT is shown in Fig. 1, which has the same configuration of the fabricated device. It was fabricated in a bottom gate contact configuration by following these steps. First, 100 nm of Chromium (Cr) were deposited on the substrate. Second, the Cr film was patterned to define the gate contact. Third, 90 nm of hafnium oxide (HfO_2) were deposited as gate dielectric. Then the PbS thin film was deposited by the CBD technique. After that, PbS and HfO_2 films were patterned and etched. Finally, 100 nm of gold (Au) were deposited and patterned to form the source and drain contacts. This process yields devices with channel widths (W) of 40, 80, and 160 μm and channel lengths (L) of 20, 40 and 80 μm. The detailed fabrication information of the p-type poly-PbS TFTs can be found in the literature [8]. However, in this work only the results of a TFT with W = 40 μm and L = 20 μm are reported. Also, the geometrical and technological parameters of simulated poly-TFT are listed in Table 1.

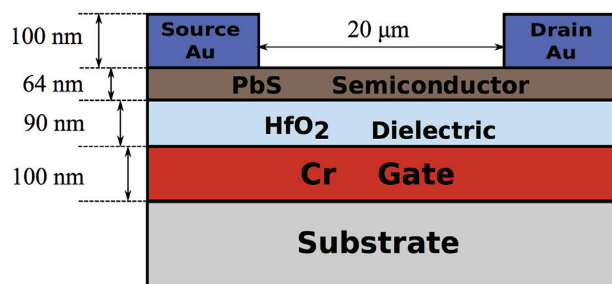

Figure 1: Cross section of PbS TFT simulated whit W=40 and L=20 μm. We used Cr as gate metal, HfO_2 as dielectric, and Au as source - drain contacts.

2.1. Simulation Method

In this study the spatially uniform DDS method was adopted [10, 11]. It considers a polycrystalline PbS film as a homogenous material with an effective density of trapping states, which are uniformly distributed throughout the semiconductor layer of PbS. The advantage of this method is that it avoids complex mesh definitions of multigrain structures, which require the knowledge of the grain size. If the transistor has a long channel (>10μm), this method will be effective for simulations of poly-TFTs due to the large number of grains and grain boundaries. For instance, the thin PbS films used in the device fabrication have an average grain size of (~ 22nm) [8]. It results in the closely spaced grain boundary regions with increased defect densities and domination of carrier dynamics in the intergrain regions over the intragrain monocrystalline effects in the carrier transport. For this reason, the thin film of poly-PbS can be considered as a homogenous material with approximately uniformly distributed defect states.

Table 1: Device Parameters used in Simulation.

Parameter	Value
Channel length L (μm)	20
Channel width W (μm)	40
Gate oxide thickness t_{ox} (nm)	90
PbS thickness (nm)	64
Energy gap at 300 K (eV)	0.37
Dielectric constant	175
Low field hole mobility (experimental) (cm^2 /Vs)	0.09
Low field hole mobility (optimized) (cm^2 /Vs)	0.064
Gate workfunction ϕ_{ms} (eV)	4.4
Density of acceptor-like tail states N_{TA} (cm^{-3}/eV)	1.74×10^{21}
Density of donor-like tail states N_{TD} (cm^{-3}/eV)	2.38×10^{17}
Density of acceptor-like Gaussian states N_{GA} (cm^{-3}/eV)	4.35×10^{18}
Density of donor-like Gaussian states N_{GD} (cm^{-3}/eV)	2.04×10^{18}
Decay energy for acceptor-like tail states W_{TA} (eV)	0.0041
Decay energy for donor-like tail states W_{TD} (eV)	0.0104
Decay energy for acceptor-like Gaussian W_{GA} (eV)	0.0054
Decay energy for donor-like Gaussian W_{GD} (eV)	0.0040
Energy of Gaussian for acceptor-like states E_{GA} (eV)	0.20
Energy of Gaussian for donor-like states E_{GD} (eV)	0.20

2.2. Optimization Method

In the context of nonlinear least squares data fitting, the objective is to estimate a set of parameters $\theta = \{\theta_1, \ldots, \theta_m\}$ which minimizes the residual between the measured or experimental data *y*(*x*) and the predicted data $f(x;\theta)$

$$F(\theta) = \frac{1}{2}\sum_{i=1}^{n}\left(y_i - f(x_i;\theta)\right)^2$$

In particular the eval function $f(x;\theta)$ correspond to the numerical solution of the partial differential equation (PDE) of the simulator Atlas/Silvaco. The above equation can be generalized for multiple curve responses case; however, a simple notation was kept for simplicity. T he numerical determination of the set of parameters θ which minimizes F(θ) corresponds to the iterative Levenberg-Marquardt (LM) algorithm

$$\left(J^T J + \lambda I\right)\delta\theta = -J^T r \tag{1}$$

where *J* is the Jacobian matrix of derivatives of the residuals with respect to the parameters θ, the residual vector is *r*, the matrix identity is *I*, and the adaptive damping parameter is λ. The above procedure is a standard numerical scheme used to perform nonlinear data fitting, where the convergence properties relationship with the steepest descent and Gauss-Newton method are understood [12].

The Silvacos manuals do not explain how they code the LM algorithm; however, it is understandable that they employ finite dfferences schemes to approximate the partial derivatives on the Jacobian matrix. Besides, in modern computer simulators, each numerical solver are coded independently, this is the case on the Atlas/Silvaco tool, where the communication between the LM algorithm and the PDEs solver is achieved through files. Furthermore, at each time that the calculation of Jacobian or the residual evaluation is needed, it is required to solve numerically the PDEs, where the parameters are taken from a given data file. So, this procedure is general, and allows the interchange of numerical solvers without modify the rest of the programs.

3 Trap Density in poly-PbS Thin Film

A poly-PbS film consists of a number of small crystalline grains with boundaries. As mentioned before, this kind of materials contains a large number of defect states within the band gap of the material. Compared with the crystalline TFT, a much higher density of trap charge in poly-PbS dominates the Poisson's equation even when these devices work under the above threshold region [13]. In narrow gap materials, as PbS, the defects arise from variation in bond lengths, grain boundaries, dangling bonds (vacancies) and other microscopic point defects. The trap states exist within the crystal grains, but many are located at the front and back oxide interfaces and the grain boundaries [14]. Moreover, experimental methods reveal that the Gaussian (deep level) gap state exhibits distinctly a peak structure in some amorphous and polycrystalline oxide semiconductor [15].

Each kind of defect plays an important role in many electrical properties in semiconductors, serving as a scattering and/or a recombination center during transport. But also the vacancies, for example, acting as largely uncontrolled dopants and having the effect

on electron and hole mobilities [16]. Therefore, in order that the performance of TFTs based on chalcogenides thin films by CBD technique could be improved, the study of the native defects in the deposited thin films is undisputed.

3.1. Density of States Model

The total DDS distribution of trapping states $g(E_t)$ in the polycrystalline PbS films is taken to be composed of four bands: two tail bands (a donor-like valence band, $g_{TD}(E_t)$ and an acceptor-like conduction band, $g_{TA}(E_t)$), and two deep Gaussian level bands (one acceptor-like, $g_{GA}(E_t)$ and the other donor-like, $g_{GD}(E_t)$) by

$$g(E_t) = g_{TD}(E_t) + g_{TA}(E_t) + g_{GA}(E_t) + g_{GD}(E_t) \quad (2)$$

$$g_{TA}(E_t) = N_{TA} exp\left(\frac{E_t - E_c}{W_{TA}}\right) \quad (3)$$

$$g_{TD}(E_t) = N_{TD} exp\left(\frac{E_v - E_t}{W_{TD}}\right) \quad (4)$$

$$g_{GA}(E_t) = N_{GA} exp\left[-\left(\frac{E_{GA} - E_t}{W_{GA}}\right)^2\right] \quad (5)$$

$$g_{GD}(E_t) = N_{GD} exp\left[-\left(\frac{E_t - E_{GD}}{W_{GD}}\right)^2\right] \quad (6)$$

where E_t is the energy of trap, Ec is the conduction band energy, Ev the valence band energy and, the subscripts (T, G, A, D) stand for tail, Gaussian (deep level), acceptor- and donor-like trap states, respectively.

The donor-like traps are positively charged (cation vacancy); therefore, they can only capture electrons. They are positive when unoccupied by an electron, but they are neutral when occupied. On the other hand, acceptor-like traps are negatively charged (anion vacancy); therefore, they can only emit an electron. They are negative when occupied, but they are neutral when unoccupied. The capture and emission processes are predicted by Atlas simulator using the Shockley-Read-Hall (SRH) recombination model.

In the steady-state, the probability of occupation of a trap level at energy E_t for the tail and deep states is given by Fermi-Dirac (FD) occupation function [17]. The total trap charge $QT = q(n_T - p_T)$ is evaluated in Atlas by following these steps. First, the density of ionized acceptor- and donor-like states is simply the product of $g(E_t)$ and the FD occupation function. Then this product is integrated to obtain the density of carriers (nT and p_T) over all possible energies within a band gap. Finally, the total trap charge Q_T obtained is subtracted from the right hand side of Poisson's equation. Q_T is also used to modify the standard SHR model in order to account for electrons and holes being emitted and captured by the acceptor and donor-like traps.

4 Simulation Results

The 2D numerical simulations of p-type PbS poly-TFT device were performed with Atlas/Silvaco simulator. The iterative Marquart algorithm (1) was used to determine the parameters N_{TA}, N_{TD}, N_{GA}, N_{GD}, W_{TA}, W_{TD}, W_{GA} and W_{GD} of the DDS model (2)-(6) numerically. So, it was necessary to propose the initial, maximum and minimum values of each parameter. These values were proposed according to the data reported by some authors that analyze the electronic properties of nanocrystalline PbS films where the DDS is extracted from experimental data [18, 19, 20]. As a result, the set of parameters, which best fit the experimental drain current (I_{DS}) of p-type TFT as function of both drain-source voltage V_{DS} and gate-source voltage VGS were obtained and are listed in Table 1.

The example of simulated and measured I_{DS} - V_{DS} output characteristics after the optimization of DDS model are displayed on Fig. 2. Having in mind the large tolerances in physical and geometrical parameters of experimental devices obtained from fabrication process, a good agreement between simulated and measured results is achieved in Fig. 2. The optimized simulation results indicate that the spatially uniform DDS method with simplified mesh generation is suitable choice for numerical simulations of long channel and thin film poly-PbS TFTs.

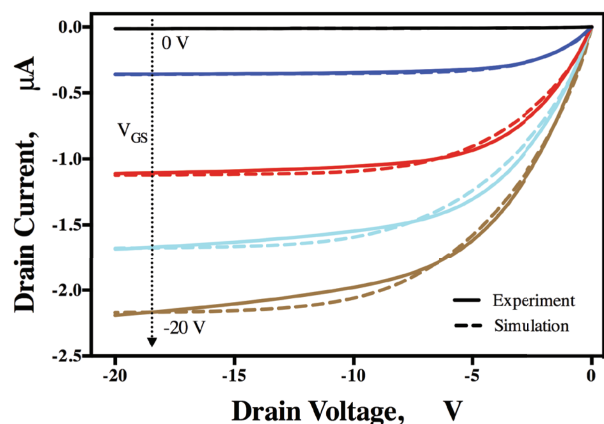

Figure 2: Simulated and experimental I_{DS}-V_{DS} characteristics of poly-PbS TFT device.

The optimized tail and deep density distributions of acceptor- and donor- like trap states for the simulated poly-PbS TFT are depicted in Fig. 3. As can be seen the density profile of defects across the forbidden gap of poly-PbS has a shape of two tail band edges and two deep levels near the midgap. The exponential band tails stem from the structural disorder in the lattice while the deep defect bands arise from impurities. Deep defects are very important for narrow band gap semiconductors [21]. The impurities and native point defects (vacancies and interstitials) are largely associated to deep traps. The deep levels can capture holes or electrons and hence acts as an electron/hole trap, which clearly affects the device performance. Fig. 3 shows that Gaussian (deep) defect bands of poly-PbS film have a peak structure, which agree with the study presented in [15].

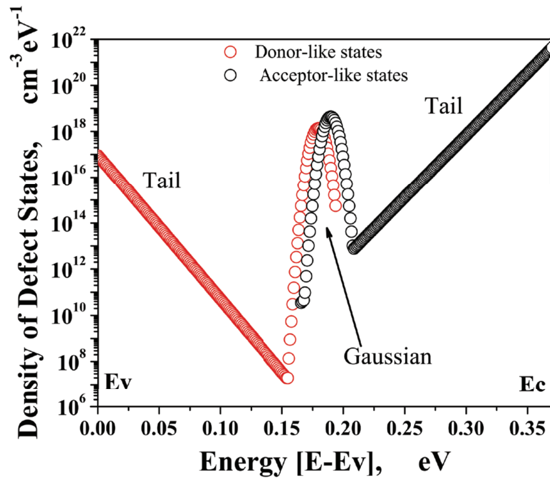

Figure 3: Optimized tail and Gaussian density distributions of acceptor- and donor-like trap states in poly-PbS TFT.

The energy-band diagram for p-type PbS MOS structure under thermal equilibrium V_{GS} = 0 (a) and accumulation regime V_{GS} < 0 (b) is shown in Fig. 4. If V_{GS} = 0 the semiconductor Fermi level E_F is near valence band and from Fig. 3 can be seen that the charge neutrality level (CNL) (the crossing point at which acceptor- and donor-like densities of states are equal) is located near midgap. For V_{GS} < 0, the bands bend upwards, drawing CNL away from E_F as shown in Fig. 4(b). As can be seen E_F lies below CNL, and ionized empty deep donor-like states build up a large positive interface charge. That is, the FD function of deep donor-like trap, which means the probability that the trap is not occupied by an electron, is increased as negative V_{GS} increases. Moreover, theorical results of [22] predict that S vacancies (acceptor-like traps) act as n-type PbS, whereas Pb vacancies (donor-like traps) act as p-type PbS.

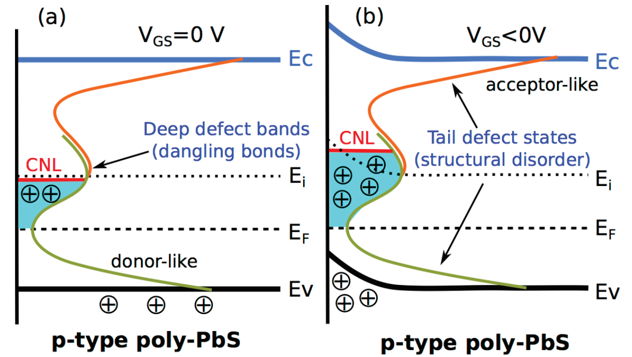

Figure 4: Energy band diagram drawn in scale for p-type PbS MOS structure (a) for $V_G = 0V$ and (b) for $V_G < 0$ (accumulation regime). Here, only the semiconductor and the interface with the oxide insulator are shown.

In Fig. 5 we display the simulated hole mobility (μ_p) as a function of transverse electric field ($E_\perp$) and V_{DS} (inset). We can notice that μp shows a strong dependence on $E_\perp$ and it is considerably lower than the mobility of crystalline TFTs. This behavior can be explained by considering that for a small negative *VGS* most of the charges are trapped. When V_{GS} becomes more negative, eventually more trap states become ionized (see Fig. 4). In this situation the effect of traps vanishes and the mobility remains almost constant with negative V_{GS}. The inset of Fig. 5 shows μ_p as a function of V_{DS} at different V_{GS} (-5V, -10V, -15V and -20V). It can be seen that μ_p has the correct behavior and it is well predicted by Atlas simulator. Both experimental and optimized (simulation) low field hole mobilities (μ_{p0}) are shown in Table 1.

In Fig. 4 is shown that tail donor-like states are located under E_F. So, they are occupied by an electron, and they are neutral; similarly, tail acceptor-like states are located above the E_F. So, they are unoccupied, and they are also neutral. So, in p-type PbS TFTs deep density states play an important role in charge transport [23]. For this reason, only the effect of different values of Gaussian density states on the transfer characteristics of the poly-PbS TFT simulated are shown in Figs. 6 and 7. As mentioned before, under low negative V_{GS}, most of the induced charge is trapped in deep states, the dominant term in Poisson equation is the density of traps n_{deep} and p_{deep}. Therefore, the sub-threshold characteristic of poly-PbS TFT can be improved by reducing both density of deep states and film thickness.

As the deep acceptor-like traps were increased, the states of electron capture (minority carriers) are increased and they cause less leakage current (see Fig. 6). Nevertheless, no significant change was observed in transfer characteristics of TFT when the deep acceptor-like traps were reduced. Accordingly, the effect of acceptor-like traps is less important in a p-type poly-PbS

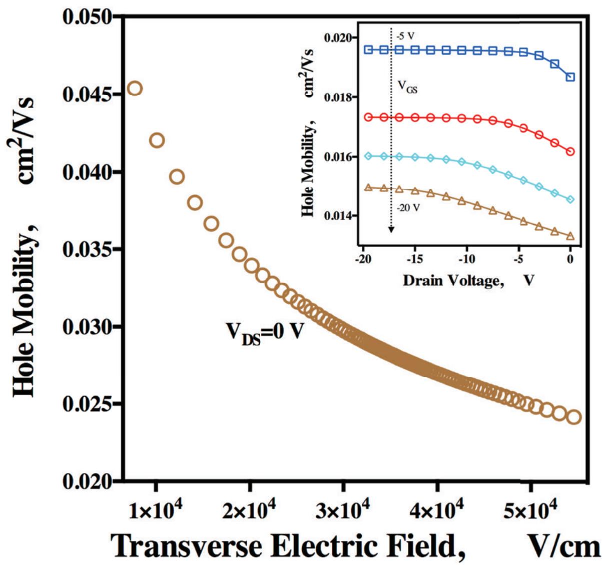

Figure 5: Hole mobility as a function of transverse electric field obtained from Atlas simulator. The inset compares the dependence of V_{DS} on hole mobility at different values of V_{GS}.

TFT in the accumulation regime. On the other hand, larger deep donor-like traps means larger positive ionized states. Notice that this situation states both less holes and less mobility in the channel (see Fig. 7). Furthermore, the total current of poly-PbS TFT is reduced. Whether the deep donor-like traps are reduced, the total current is increased, yet the V_{TH} shifts to positive values. Moreover, although the experimental and simulated value of V_{TH} is positive, it should be negative (accumulation regime). A similar conclusion about the effect of deep traps on V_{TH} behavior is presented in [24] for TFTs with cadmium sulfide (CdS) films, as

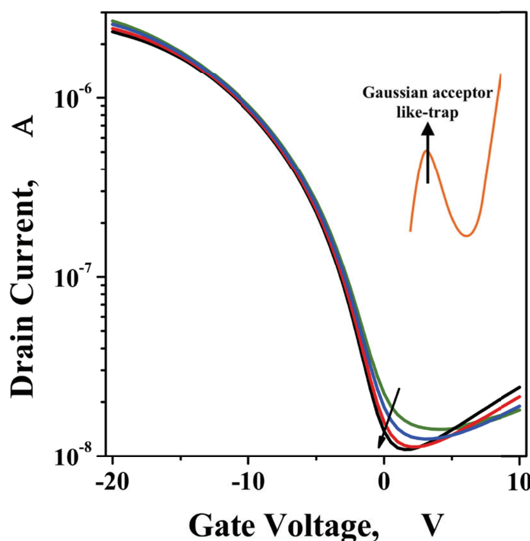

Figure 6: Transfer characteristics of the poly PbS TFT simulated as a function of V_{GS} for different values of deep acceptor-like traps (increased).

active channel, deposited by CBD technique. Because the deep traps affect the device performance by either doping the PbS film or acting as trap sites, both acceptor- and donor-like traps should be controlled in order to improve the p-type poly-PbS TFT electrical characteristics.

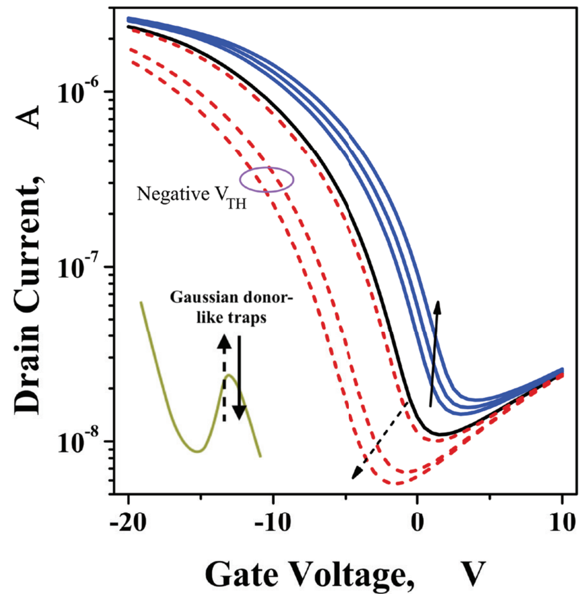

Figure 7: Transfer characteristics of the poly PbS TFT simulated as a function of V_{GS} for different values of deep donor-like traps (increased and reduced).

Fig. 3 shown that the point defects act as deep traps states situated at different energy depths within the forbidden gap, thereby influencing the principal parameters of poly-PbS TFTs (V_{TH} , mobility, I_{on} /I_{off} ratio and mobile charge density). It is demonstrated that after thermal annealing the electrical properties of thin films deposited by CBD are improved [8, 24]. This is attributed to the change in larger grain size, lattice parameter and crystalline structure along with a reduction of defects. Nevertheless, some defects are still present in the thin film and longer annealing times might be necessary to eliminate the vacancies or interstitials. In addition, a significant amount of S or Pb (anion or cation) vacancies could be created in the PbS films as function of the environment used during the synthesis, sulfur-poor or lead-poor. Also, the velocity of ions in a solution should be considered in order to control the S and Pb vacancies in the thin films deposited by CBD technique.

5 Conclusions

To sum up, the p-type PbS poly-TFT's electrical characteristics can be predicted with physically based two-dimensional device simulator Atlas using the embedded

density of defect models. The spatially uniform density of defect states method used for trapped charge evaluation and the parameter optimization of density defect model give a good agreement between simulated and experimental characteristics. Also, it is clear that the deep density of states in poly-PbS band gap affects the electrical characteristics of p-type TFTs. The high density of deep donor-like states (cation vacancies) found to be degrading device performance while it is not a concern for deep acceptor-like states (anion vacancies). The cation vacancies act as a deep electron donor, which affect the p-type device performance. To optimize the design of p-type PbS poly-TFTs both anion and cation vacancies should be controlled. These findings are important for the better understanding of TFTs based on calchogenides materials deposited by chemical bath deposition technique.

6 References

1. Z. Meng, M. Wang, M. Wong, High performance low temperature metal-induced unilaterally crystallized polycrystalline silicon thin film transistors for system-on-panel applications, IEEE Transactions on Electron Devices 47 (2) (2000) 404–409. doi:10.1109/16.822287.
2. S. Zhang, C. Zhu, J. K. O. Sin, J. N. Li, P. K. T. Mok, Ultra-thin elevated channel poly-si tft technology for fully-integrated amlcd system on glass, IEEE Transactions on Electron Devices 47 (3) (2000) 569–575. doi:10. 1109/16.824731.
3. H. W. Zan, S. C. Kao, The effects of drain-bias on the threshold voltage instability in organic tfts, IEEE Electron Device Letters 29 (2) (2008) 155–157. doi:10.1109/LED.2007.914081.
4. A. Obaid, M. Mahdi, Y. Yusof, M. Bououdina, Z. Hassan, Structural and optical properties of nanocrystalline lead sulfide thin films prepared by microwave-assisted chemical bath deposition, Materials Science in Semiconductor Processing 16 (3) (2013) 971 – 979. doi:http://dx.doi.org/10.1016/j.mssp.2013.02.005. URL http://www.sciencedirect.com/science/article/pii/S1369800113000413
5. V. Stancu, M. Buda, L. Pintilie, I. Pintilie, T. Botila, G. Iordache, Investigation of metal-oxide semiconductor field-effect transistor-like si/sio2/(nano)crystalline pbs heterostructures, Thin Solid Films 516 (12) (2008) 4301 – 4306. doi:http://dx.doi.org/10.1016/j.tsf.2007.11.116. URL http://www.sciencedirect.com/science/article/pii/S0040609007019682
6. G. P. Agrawal, N. K. Dutta, Semiconductor Lasers, 2nd Edition, Kluwer Academic, 1995.
7. T. K. Chaudhuri, A solar thermophotovoltaic converter using pbs photovoltaic cells, International Journal of Energy Research 16 (6) (1992) 481–487. doi:10.1002/er.4440160605. URL http://dx.doi.org/10.1002/er.4440160605
8. A. Carrillo-Castillo, A. Salas-Villasenor, I. Mejia, S. Aguirre-Tostado, B. Gnade, M. Quevedo-Lpez, P-type thin films transistors with solution-deposited lead sulfide films as semiconductor, Thin Solid Films 520 (7) (2012) 3107 – 3110. doi:http: //dx.doi.org/10.1016/j.tsf.2011.12.016. URL http://www.sciencedirect.com/science/article/pii/S0040609011021183
9. G. Fortunato, P. Migliorato, Determination of gap state density in polycrystalline silicon by fieldeffect conductance, Applied Physics Letters 49 (16) (1986) 1025–1027. doi:http://dx.doi.org/10.1063/1.97460. URL http://scitation.aip.org/content/aip/journal/apl/49/16/10.1063/1.97460
10. M. D. Jacunski, M. S. Shur, M. Hack, Threshold voltage, field effect mobility, and gate-to-channel capacitance in polysilicon tfts, IEEE Transactions on Electron Devices 43 (9) (1996) 1433–1440. doi:10.1109/16.535329.
11. Y. Z. Xu, F. J. Clough, E. M. S. Narayanan, Y. Chen, W. I. Milne, Turn-on characteristics of polycrystalline silicon tft's-impact of hydrogenation and channel length, IEEE Electron Device Letters 20 (2) (1999) 80–82. doi:10.1109/55.740658.
12. J. Nocedal, S. Wright, Numerical Optimization, Springer Series in Opera- tions Research and Financial Engineering, Springer New York, 2006. URL https://books.google.com.mx/books?id=eNlPAAAAMAAJ
13. Y. Liu, R. h. Yao, B. Li, W. L. Deng, An analytical model based on surface potential for a-si:h thin-film transistors, Journal of Display Technology 4 (2) (2008) 180–187. doi:10.1109/JDT.2007.907122.
14. M. Kimura, Evaluation of trap states at front and back oxide interfaces and grain boundaries using electrical characteristic analysis and device simulation of polycrystalline silicon thin-film transistors, Electronics and Communications in Japan (Part II: Electronics) 88 (2) (2005) 1–10. doi:10.1002/ecjb.20124. URL http://dx.doi.org/10.1002/ecjb.20124
15. H.-H. Hsieh, T. Kamiya, K. Nomura, H. Hosono, C.-C. Wu, Modeling of amorphous ingazno4 thin film transistors and their subgap density of states, Applied Physics Letters 92 (13). doi:http://dx.doi.org/10.1063/1.2857463. URL http://scitation.aip.org/content/aip/journal/apl/92/13/10.1063/1.2857463
16. S. Ahmad, S. D. Mahanti, K. Hoang, M. G. Kanatzidis, *Ab initio* studies of the electronic structure

of defects in pbte, Phys. Rev. B 74 (2006) 5205. doi:10.1103/PhysRevB.74.155205.

17. S. Sze, K. Ng, Physics of Semiconductor Devices, Wiley, 2006. URL https://books.google.es/books?id=o4unkmHBHb8C
18. Z. Jin, A. Wang, Q. Zhou, Y. Wang, J. Wang, Detecting trap states in planar pbs colloidal quantum dot solar cells, Scientific Reports 6 (3) (2016)569–575. doi:http://dx.doi.org/10.1038/srep37106.
19. N. MI, H. R, W. S, M. H, S. M, H. W, T. J, L. MA, Broadening of distribution of trap states in pbs quantum dot field-effect transistors with high-k dielectrics, ACS Appl Mater Interfaces 9 (5) (2017) 4719–4724. doi:http://dx.doi.org/10.1021/acsami.6b14934.
20. N. MI, H. R, W. S, M. H, S. M, H. W, T. J, L. MA, High mobility and low density of trap states in dual-solid-gated pbs nanocrystal field-effect transistors, Advanced Materials 27 (12) (2015) 2107–2112. doi:http:// dx.doi.org/10.1002/adma.201404495.
21. S. Mahanti, K. Hoang, S. Ahmad, Deep defect states in narrow band-gap semiconductors, Physica B: Condensed Matter 401402 (2007) 291 – 295, proceedings of the 24th International Conference on Defects in Semiconductors. doi:http://dx.doi.org/10.1016/j.physb.2007.08.169. URL http://www.sciencedirect.com/science/article/pii/S0921452607007168
22. D. Zong-Ling, X. Huai-Zhong, X. Sheng-Lan, H. Yan, C. Xiao-Shuang, First-principles study of electronic properties in pbs($\bar{1}$00) with vacancy defect, Chinese Physics Letters 24 (11) (2007) 3218. URL http://stacks.iop.org/0256-307X/24/i=11/a=054
23. P. Nagpal, V. I. Klimov, Role of mid-gap states in charge transport and photoconductivity in semiconductor nanocrystal films, Nature Communications 2 (486). doi:http://dx.doi.org/10.1038/ncomms1492.
24. A. L. Salas-Villasenor, I. Mejia, M. Sotelo-Lerma, Z. B. Guo, H. N. Alshareef, M. A. Quevedo-Lopez, Improved electrical stability of cds thin film transistors through hydrogen-based thermal treatments, Semiconduc- tor Science and Technology 29 (8) (2014) 085001. URL http://stacks.iop.org/0268-1242/29/i=8/a=085001

Arrived: 22. 12. 2016
Accepted: 03. 05. 2017